ISSN 0208-7774 TRIBOLOGIA 2/2018 p. 5–12

Henryk BĄKOWSKI*

ESTIMATION OF THE WEAR MECHANISM IN SLIDING CONTACT OF SATELITE GEARS OF A HYDRAULIC MOTOR

OCENA ZUŻYCIA MECHANIZMU SATELITOWEGO W SKOJARZENIU ŚLIZGOWYM WYKORZYSTYWANEGO W SILNIKU HYDRAULICZNYM

Key words: wear, sliding contact, hydraulic motor.

Abstract The paper presents tests of the wear of selected elements of a hydraulic satellite engine in sliding contact. The tests were carried out on the tribotester T-05 in a roll-block system, taking into account the influence of the most important operational parameters determining the durability of the friction node in question. The performed tribological, metallographic and profilographometric studies allowed the comparison and evaluation of the mechanism of sliding contact wear in the laboratory stand and on the real object, which allows one to make far-reaching assumptions about the durability of the contact in question and its resistance to wear under various operating.

Słowa kluczowe: zużycie, skojarzenie ślizgowe, silnik hydrauliczny.

Streszczenie W pracy przedstawiono badania zużycia wybranych elementów hydraulicznego silnika satelitowego w skojarzeniu ślizgowym. Badania przeprowadzono na tribotesterze T-05 w układzie rolka-klocek, uwzględniając wpływ najważniejszych parametrów eksploatacyjnych decydujących o trwałości rozpatrywanego węzła tarcia. Przeprowadzone badania tribologiczne, metalograficzne i profilografometryczne pozwoliły na porównanie i ocenę mechanizmu zużywania skojarzenia ślizgowego na stanowisku laboratoryjnym i na obiekcie rzeczywistym, co pozwala wysuwać daleko idące przypuszczenia co do trwałości rozpatrywanego skojarzenia i jego odporności na zużycie w różnych warunkach eksploatacji.

INTRODUCTION

The operation of the satellite engine's operating mechanism is based on the cooperation of a small element with external teeth, called the planet, with a non-round gear element with internal teeth, called the bypass, with the help of satellites placed between them. Satellites play the role of mobile, sealed divisions between the ventricles. At the same time, they function as supply and outflow dividers by closing the respective openings in the side plates with their face at the moment of the passage of a given chamber from the filling phase into the extrusion phase. The correct course of filling the operating chambers of the satellite mechanism ensures timing. The timing is made of S-satellites and the inflow openings IH and the OH outflow in the timing plates CP. During the operation of the mechanism, the satellites move relative to the planet and bypass, respectively covering and revealing the inflow openings IH or exposing the drain holes OH in the CP plates. The satellite mechanism can be used to build both a hydraulic motor and a pump in various hydraulic drives, especially in the mining industry **[L. 1, 2]**.

---

* Silesian University of Technology, Faculty of Transport, ul. Z. Krasińskiego 8, 40-019 Katowice, Poland, e-mail: henryk.bakowski@polsl.pl.

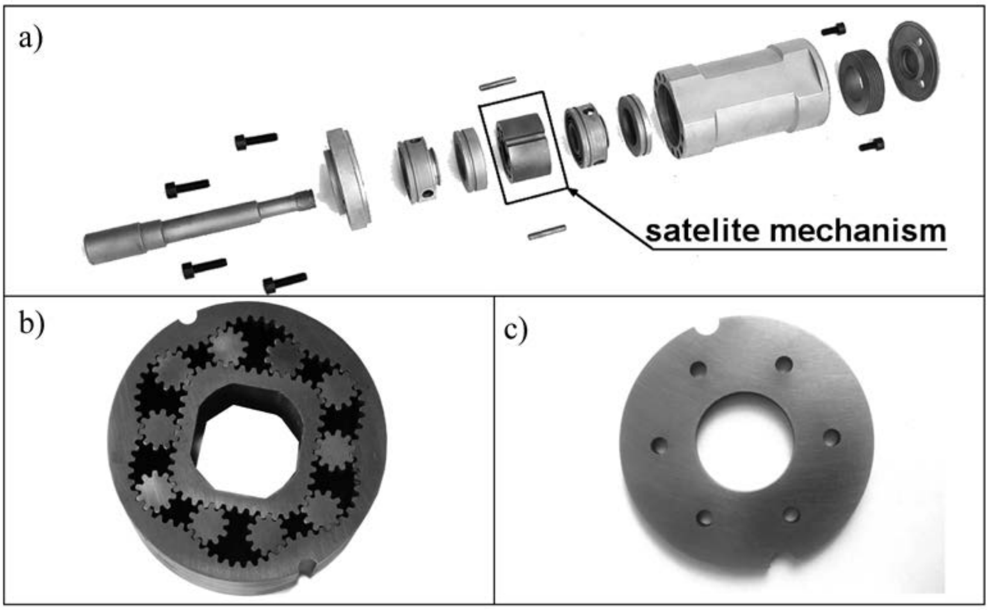

Fig. 1. **View of the hydraulic engine [2]: a) unfolded, b) satellite mechanism, c) compensation / timing plate**
Rys. 1. Widok silnika hydraulicznego [2]: a) w rozłożeniu, b) mechanizm satelitowy, c) płytka kompensacyjna/rozrządu

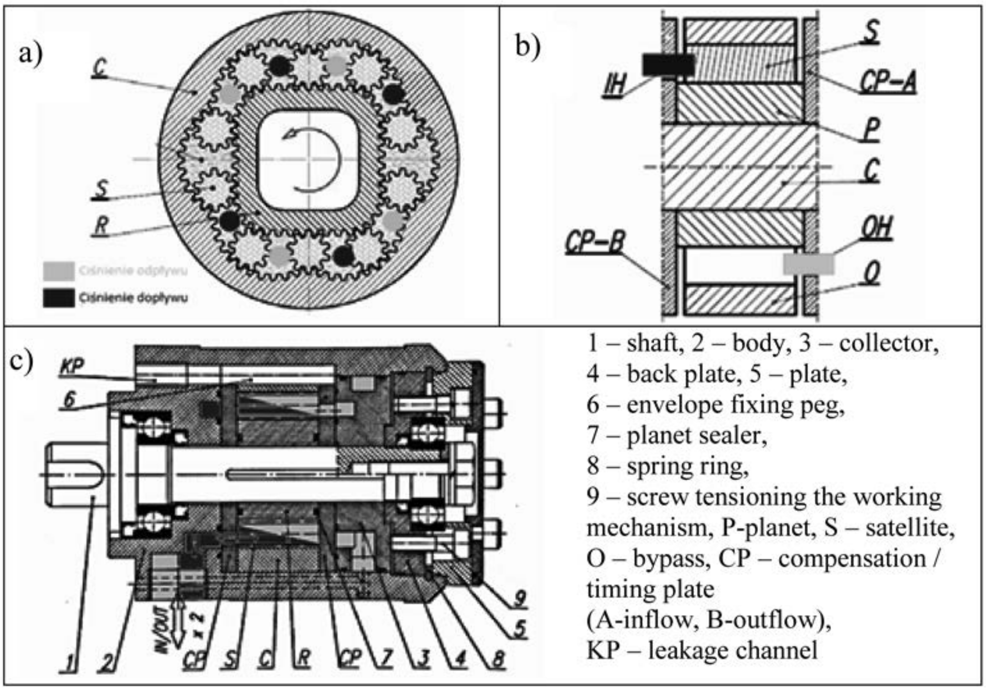

Fig. 2. **Satellite mechanism: a) view, b) cross-section of the satellite mechanism, c) cross-section of the engine [L. 1, 3]**
Rys. 2. Mechanizm satelitowy: a) widok, b) przekrój mechanizmu satelitowego, c) przekrój silnika **[L. 1, 3]**

The main assumption in the subject was to determine the impact of operating conditions on selected tribological properties of sliding contact, and thus, on the assessment of the wear of the tested system. The critical places determining the efficiency and correct operation of the hydraulic machine is to provide compensation for axial clearances and the appropriate and unchangeable shape of the cooperating teeth in time. The task of compensating the axel is to limit leaks on faces of working elements (satellites and planets) **[L. 4]**. As a hydraulic liquid, a 1% emulsion was used (water-oil emulsion HFA), along with impurities from the normal operation of the real object **[L. 5]**.

This work determines the impact of the main operational parameters on the consumption of satellites, which causes a decrease in the efficiency of the facility (linear wear). The scope of research included the performance of wear tests at the laboratory stand, metallographic tests, both qualitative and quantitative, as well as profilometric tests. In addition, examples of vibro-acoustic tests were presented (**Figure 3b**).

METHODOLOGY OF TESTS AND MEASUREMENT TECHNIQUE

The tests were carried out on a T-05 laboratory bench in a roll-block system. As a sample, the material used for satellites had the designation EN-40CrMnNiMo8-6-4, while bearing steel (100Cr6) of comparable hardness with the hardness of the timing plate was used for the counter-sample. **Table 1** presents the chemical composition of the material used for satellites and strength properties (**Table 2**).

Table 1. Chemical composition of alloy steel [L. 6]
Tabela 1. Skład chemiczny stali stopowej **[L. 6]**

Chemical composition %	C	Si	Mn	Cr	Ni	Mo	S
	0.37	0.3	1.4	2.0	1.0	0.2	<0.01

Table 2. Selected mechanical properties of alloy steel [L. 6]
Tabela 2. Wybrane właściwości mechaniczne stali stopowej **[L. 6]**

Trade name of steel	Density [g/cm^3]	Hardness HB	Tensile strength; Rm, MPa	Yield strength; Re, MPa
IMPAX	7.8	330	1020	900

Table 3. Warunki badań [L. 7]
Tabela 3. Warunki badań **[L. 7]**

Operating factors	Working pressure,/load,	Rotation speed, min^{-1}	Fluid
Real object – hydraulic engine	20–28 MPa	100–500	Emulsion HFA/water
Laboratory station	5–20 N		

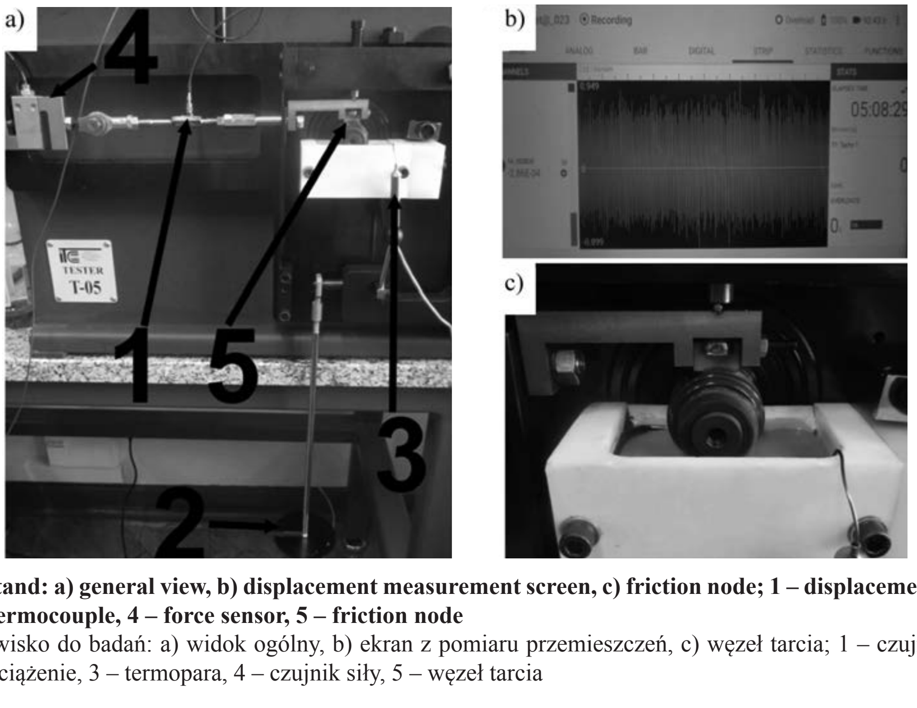

Fig. 3. Test stand: a) general view, b) displacement measurement screen, c) friction node; 1 – displacement sensor, 2 – load, 3 – thermocouple, 4 – force sensor, 5 – friction node
Rys. 3. Stanowisko do badań: a) widok ogólny, b) ekran z pomiaru przemieszczeń, c) węzeł tarcia; 1 – czujnik przemieszczeń, 2 – obciążenie, 3 – termopara, 4 – czujnik siły, 5 – węzeł tarcia

Test conditions were selected based on the actual operational parameters of the satellite hydraulic engine operating in a hard coal mine **[L. 7]**. **Table 3** presents the typical operating conditions of the satellite mechanism under consideration and the adequate values at the laboratory stand. **Figure 3** shows a photograph of the T-05 tribotester during testing, while **Figure 4** shows the solid model of the satellite mechanism.

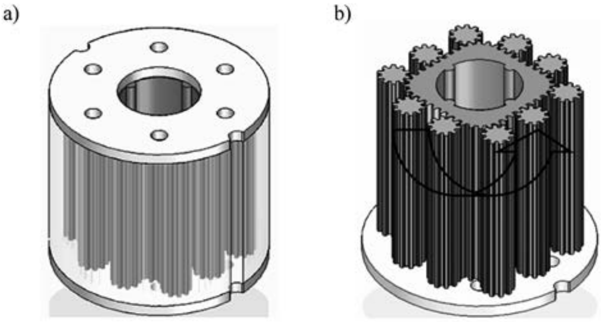

Fig. 4. The solid model of the satellite mechanism: a) complete set, b) selected elements

Rys. 4. Model bryłowy mechanizmu satelitowego: a) kompletny zespół, b) wybrane elementy

RESULTS

The tests were carried out on a stand in a roll-block system on the T-05 tribotester with the possibility of heating the lubricating medium. The results of tribological tests (mass loss) are shown in **Figure 5**.

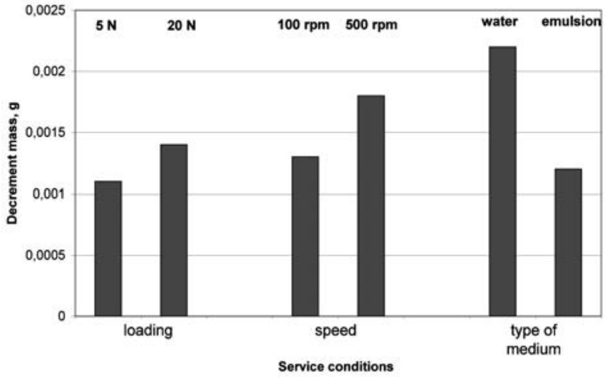

Fig. 5. Dependence of mass loss in function of selected operational factors

Rys. 5. Zależność ubytku masy w funkcji wybranych czynników eksploatacyjnych

Tribological tests allowed determining the influence of selected operational factors on wear and the coefficient of friction. Determination of the main operational factors affecting the formation of tribological properties made it possible to determine the intensity of wear and determine the type of wear based on metallographic examinations (**Figs. 5** and **7**). In the perspective, Hartley's poly-selection plan will be used with the levels accepted for testing (minimum, central and maximum) in the future.

Figure 6 shows the diagrams of the frictional resistance dependence on the number of cycles. The beginnings of the mashing phase were determined from the graphs, and the estimated results are illustrated in **Table 4**.

Table 4. List of the number of cycles at the time of obliterate depending on operational factors

Tabela 4. Zestawienie liczby cykli w chwili zatarcia w zależności od czynników eksploatacyjnych

Operating parameters	Load		Speed		Lubricating medium	
	5 N	20 N	100 min^{-1}	500 min^{-1}	water	contaminated emulsion
Number of cycles to obliterate	21000	8000	50000	80000	40000	50000

During tribological tests, the temperature in the friction node slightly increased due to the friction processes occurring in the tested sliding contact, reaching the value of 38–44ºC.

Metallographic examinations of the friction surface of the samples after cooperation were carried out. A dominating mechanism of frictional wear was observed on the surface. This is evidenced by the numerous traces of micro-scraping observed on each friction surface tested. For a larger load (20 N) adhesive surfaces appear on the friction surface, causing the breaks to appear, resulting in an irregular curve of frictional resistance and the intensification of the wear process (**Fig. 6b**). The influence of speed on wear is significant, because, at the higher speed (500 rpm), deeper and larger grooves appear on the surface as well as plastic deformations (in

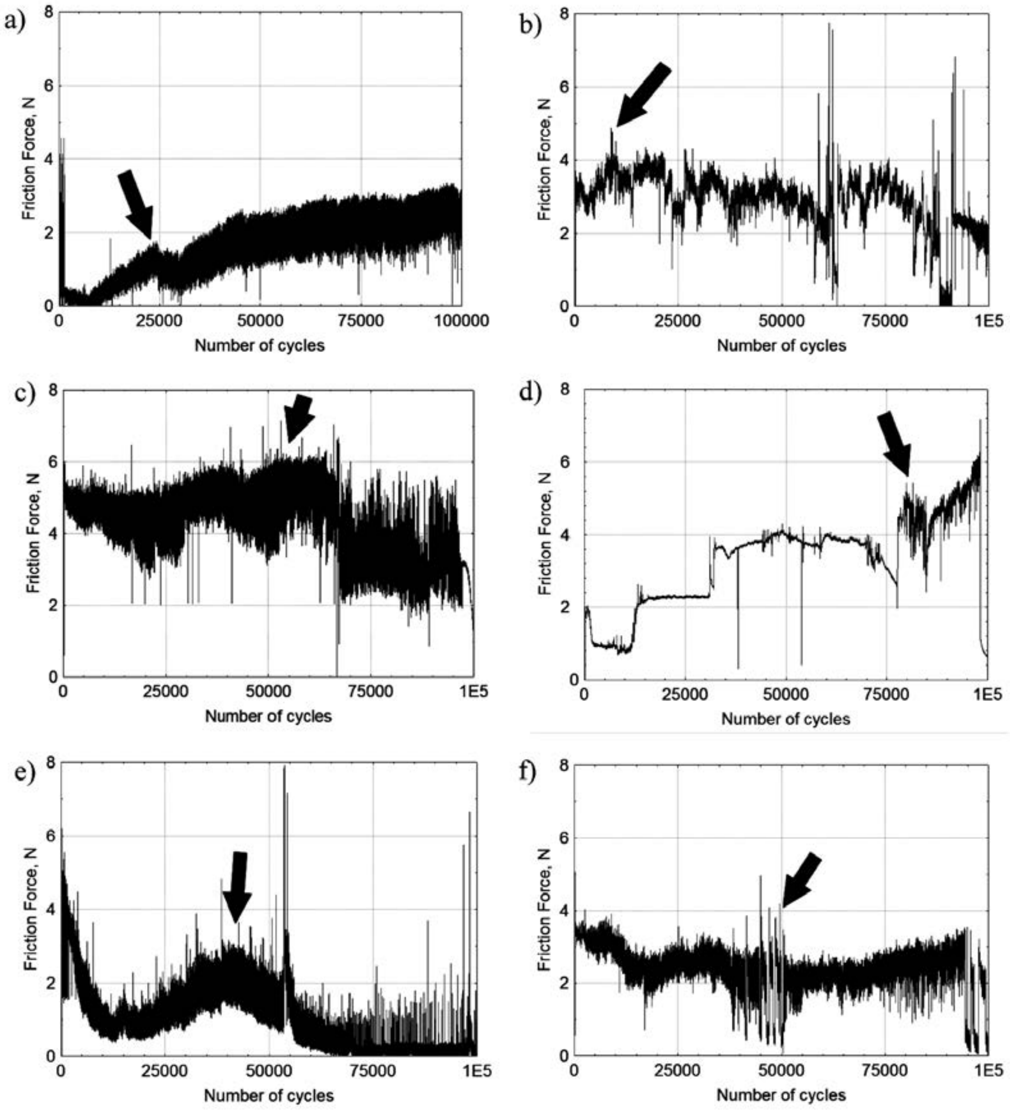

Fig. 6. Frictional resistance as a function of the number of cycles: a) for 5 N; b) for 20 N; c) for 100 rpm; d) for 500 rpm; e) in the presence of water; f) in the presence of emulsions (arrows indicate the estimated number of cycles to failure)

Rys. 6. Zależności oporów tarcia w funkcji liczby cykli: a) dla 5 N; b) dla 20 N; c) dla 100 obr./min; d) dla 500 obr./min; e) w obecności wody; f) w obecności emulsji (strzałkami zaznaczono oszacowane liczby cykli do zatarcia)

the lower part of **Fig. 7d**). Considering the influence of the lubricating medium in the form of water, it causes the occurrence of oxidation on the surface in addition to the accompanying frictional wear processes (**Fig. 7e**).

Optical profilographometer measurements were performed for the timing plate and the front surface of the satellite. The working surface of the timing plate practically showed no signs of wear (**Fig. 8**), due to the high strength properties. In contrast, numerous strands of scratches and abrasive and adhesive breaks were observed on the face of the satellite (**Figure 9**).

Comparing the mechanism of wear in the real system (timing plate-satellite) and in the laboratory stand (roll-block), a significant similarity was observed in the wear mechanism. This indicates the correct selection of the main operating parameters affecting the technical condition of the facility and the sliding contact and the testing machine itself.

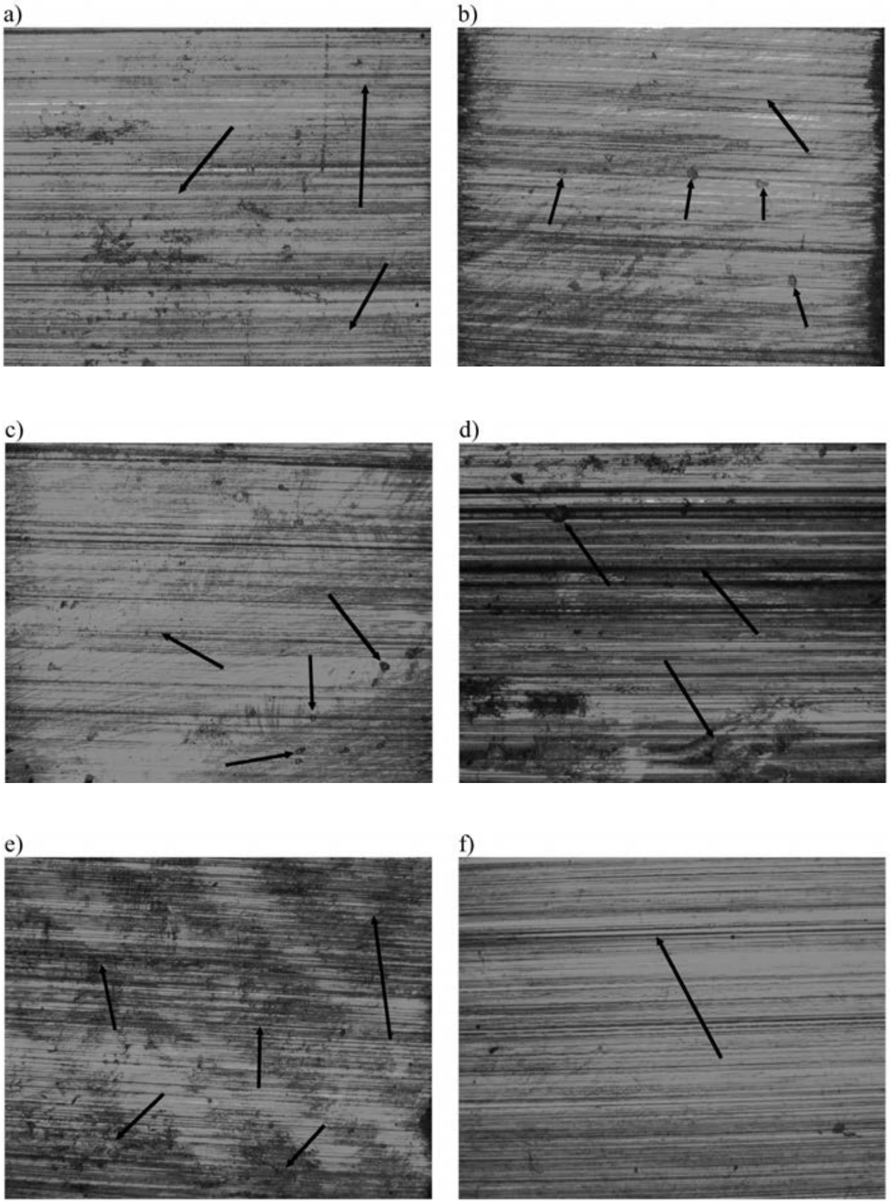

Fig. 7. Surface of friction after contact: a) for 5 N (friction wear); b) for 20 N (friction and adhesion wear); c) for 100 rpm (friction and adhesion wear); d) for 500 rpm (friction and adhesion wear with plastic deformation); e) in the presence of water (oxidation wear); f) in the presence of an emulsion (friction wear), magnification x100 (the arrows indicate the occurring surface phenomena)

Rys. 7. Powierzchnia tarcia po współpracy: a) dla 5 N; b) dla 20 N; c) dla 100 obr./min; d) dla 500 obr./min; e) w obecności wody; f) w obecności emulsji, pow. x100 (strzałkami zaznaczono występujące zjawiska powierzchniowe)

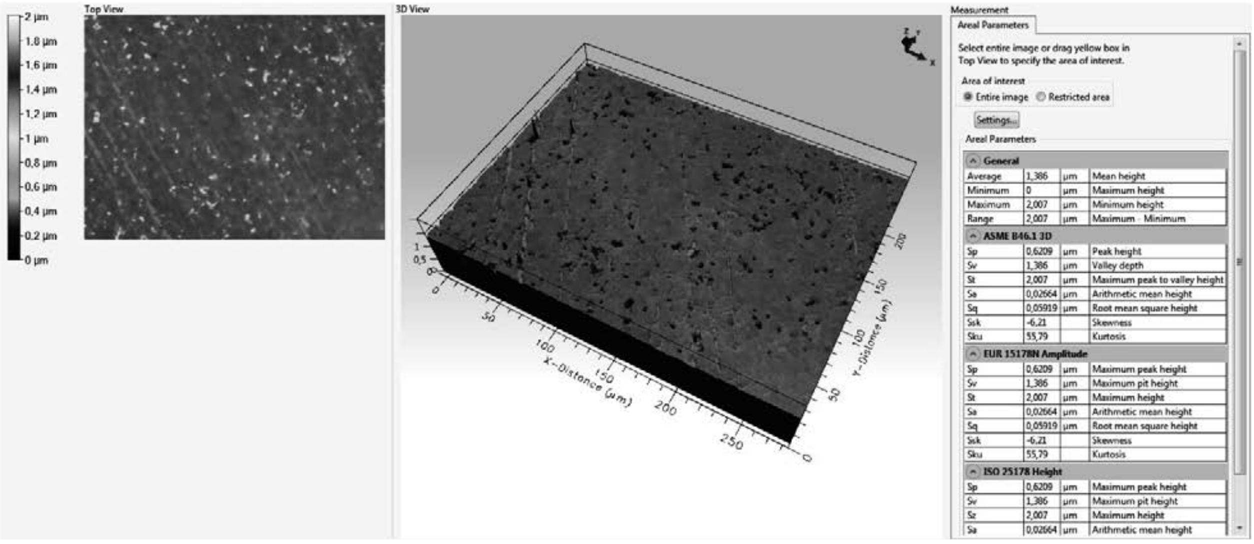

Measurement

Areal Parameters

Select entire image or drag yellow box in Top View to specify the area of interest.

Area of interest

● Entire image ○ Restricted area

Areal Parameters

General			
Average	1,386	µm	Mean height
Minimum	0	µm	Maximum height
Maximum	2,007	µm	Minimum height
Range	2,007	µm	Maximum - Minimum
ASME B46.1 3D			
Sp	0,6209	µm	Peak height
Sv	1,386	µm	Valley depth
St	2,007	µm	Maximum peak to valley height
Sa	0,02664	µm	Arithmetic mean height
Sq	0,05919	µm	Root mean square height
Ssk	-6,21		Skewness
Sku	55,79		Kurtosis
EUR 15178N Amplitude			
Sp	0,6209	µm	Maximum peak height
Sv	1,386	µm	Maximum pit height
St	2,007	µm	Maximum height
Sa	0,02664	µm	Arithmetic mean height
Sq	0,05919	µm	Root mean square height
Ssk	-6,21		Skewness
Sku	55,79		Kurtosis
ISO 25178 Height			
Sp	0,6209	µm	Maximum peak height
Sv	1,386	µm	Maximum pit height
Sz	2,007	µm	Maximum height
Sa	0,02664	µm	Arithmetic mean height

Fig. 8. Surface of the timing plate's friction after cooperation together with surface roughness parameters
Rys. 8. Powierzchnia tarcia płytki rozrządu po współpracy wraz z parametrami chropowatości powierzchni

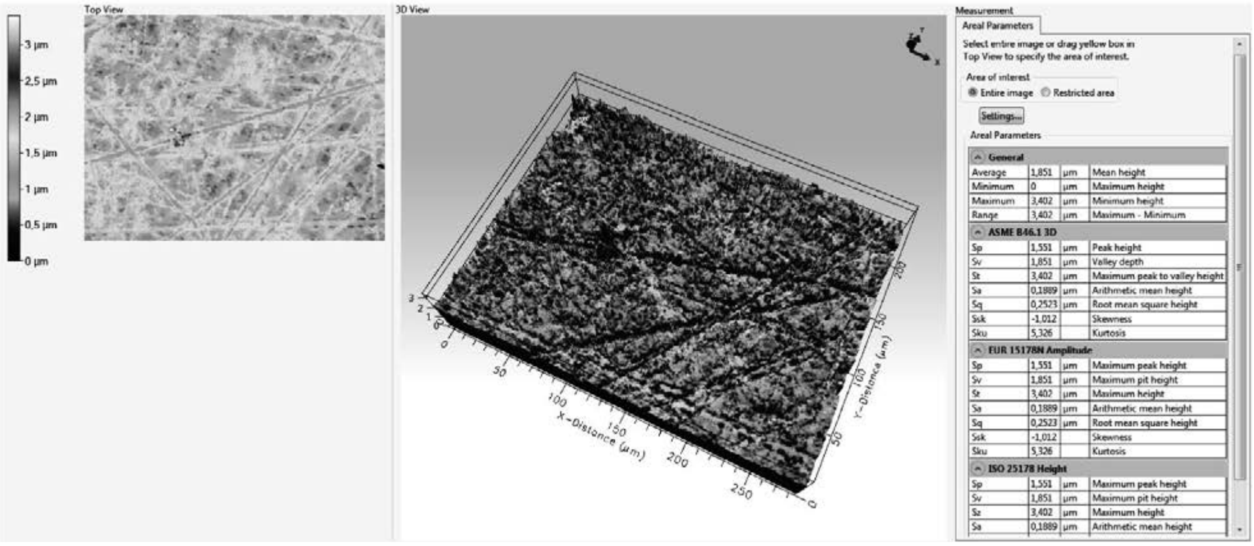

Measurement

Areal Parameters

Select entire image or drag yellow box in Top View to specify the area of interest.

Area of interest

● Entire image ○ Restricted area

Areal Parameters

General			
Average	1,851	µm	Mean height
Minimum	0	µm	Maximum height
Maximum	3,402	µm	Minimum height
Range	3,402	µm	Maximum - Minimum
ASME B46.1 3D			
Sp	1,551	µm	Peak height
Sv	1,851	µm	Valley depth
St	3,402	µm	Maximum peak to valley height
Sa	0,1889	µm	Arithmetic mean height
Sq	0,2523	µm	Root mean square height
Ssk	-1,012		Skewness
Sku	5,326		Kurtosis
EUR 15178N Amplitude			
Sp	1,551	µm	Maximum peak height
Sv	1,851	µm	Maximum pit height
St	3,402	µm	Maximum height
Sa	0,1889	µm	Arithmetic mean height
Sq	0,2523	µm	Root mean square height
Ssk	-1,012		Skewness
Sku	5,326		Kurtosis
ISO 25178 Height			
Sp	1,551	µm	Maximum peak height
Sv	1,851	µm	Maximum pit height
Sz	3,402	µm	Maximum height
Sa	0,1889	µm	Arithmetic mean height

Fig. 9. Front satellite surface after cooperation with surface roughness parameters
Rys. 9. Czołowa powierzchnia satelity po współpracy wraz z parametrami chropowatości powierzchni

CONCLUSIONS

On the basis of tribological tests carried out on a laboratory bench and on a real object as well as metallographic and profilometric studies, the following conclusions can be drawn:

- The dominant mechanism of wear in the considered friction joint in both the real and laboratory objects is abrasive wear.
- Additional wear mechanisms (adhesive and oxidation) contribute to the intensification of the wear itself.
- The type of wear depends on the load (additionally there is adhesive wear), speed (more abrasive wear and plastic deformations occurring on the surface) and lubricating medium (oxidation phenomenon).
- It is possible to estimate the failure of the tested contact depending on the value of operating parameters.
- The application of a poly-selective experiment plan that captures the impact of the above operational factors will allow forecasting and determining the service life of the hydraulic engine.

The work done in the framework of BK-241/RT1/2018.

REFERENCES

1. Śliwiński P.: Satelitowe maszyny wyporowe. Monografia. Politechnika Gdańska, 2016.
2. Szwajca T.: Silnik hydrauliczny satelitowy. Patent PL 215 061 B1.
3. Śliwiński P.: The basics of design and experimental tests of the commutation unit of a hydraulic satellite motor. Archives of civil and mechanical engineering 16 (2016), pp. 634–644.
4. Śliwiński P.: Rozrząd silnika satelitowego z obracającym się korpusem. Napędy i Sterowanie 10 (2016), pp. 98–105.
5. Śliwiński P.: Porównanie własności smarnych wody, emulsji oleju w wodzie typu HFA-E oraz oleju Total Azolla 46 jako czynników roboczych w układach hydraulicznych. Tribologia 3 (2009), pp. 257–272.
6. UDDEHOLM IMPAX® SUPREME. Karta materiałowo-technologiczna.
7. Bołoz Ł.: Pomiar parametrów wiertarki hydraulicznej i procesu wiercenia obrotowego. Napędy i Sterowanie 1 (2018), pp. 70–73.